A new meshless method for free vibration analysis of plates using radial basis function

Y. T. Lee[1], I. L. Chen[2], K. H. Chen[3], J. T. Chen[4]

[1]Graduate Student, Department of Harbor and River Engineering
National Taiwan Ocean University, Keelung, Taiwan
[2]Associate Professor, Department of Naval Architecture
National Kaohsiung Institute of Marine Technology, Kaohsiung, Taiwan
[3]Ph.D Candidate, Department of Harbor and River Engineering
National Taiwan Ocean University, Keelung, Taiwan
[4]Professor, Department of Harbor and River Engineering
National Taiwan Ocean University, Keelung, Taiwan

Abstract

In this paper, a new meshless method for solving the eigenfrequencies of plates using the radial basis function (RBF) is proposed. By employing the imaginary-part fundamental solution as the RBF, the coefficients of influence matrices are easily determined. True eigen solutions in conjunction with spurious eigen solution are obtained for plate vibration. It is found that spurious eigen solution for the simply-supported plate using the present method is the same as the true eigensolution of the clamped case in the numerical experiments. To verify this finding, the circulant is adopted to analytically derive the true and spurious eigenequation in the discrete system of a circular plate. In order to obtain the eigenvalues and boundary modes at the same time, the singular value decomposition (SVD) technique is utilized. Two examples are demonstrated analytically and numerically to see the validity of the present method.
Keywords: Meshless method; Radial basis function; Plate vibration; Clamped; Simply-supported

Introduction

Mesh generation of a complicated geometry is always time consuming in the stage of model creation for engineers in dealing with engineering problems by employing numerical methods, e.g., the finite difference method (FDM), finite element method (FEM) and boundary element method (BEM). In the last decade, researchers have paid attention to the meshless method without employing the concept of element. Several meshless methods have also been reported in the literature, for example, the domain-based methods including the element-free Galerkin method [1], the reproducing kernel method [2], and boundary-based methods including the boundary node method [3], the meshless local Petrov-Galerkin approach [4], the local boundary integral equation method [5] and the RBF approach [6].

Integral equations and BEM have been utilized to solve the boundary value problems for a long time. Several approaches, e.g., the complex-valued BEM, the method of fundamental solution, the dual reciprocity method (DRM), the particular integral method [7], multiple reciprocity method (MRM), the real-part BEM and imaginary-part BEM [8], have been developed for eigenproblems. To solve the problem by using the complex-valued BEM, the influence coefficient matrix would be complex arithematics [9]. Therefore, Tai and Shaw [10] employed only the real-part kernel to solve the eigenvalue problems and to avoid the complex-valued computation in sacrifice of appearance of spurious eigenvalues. To avoid the singular and hypersingular integrals, De Mey [11] used imaginary-part fundamental solution to solve the eigenproblems and also encountered the problem of eigen solution. Kang et al. proposed the NDIF (Non-dimensional Dynamic Influence Function) method to solve eigenproblems of membranes [12], acoustic cavities [13], and plates [14]. Later, Chen et al. commented that the NDIF method is a special case of imaginary-part BEM after lumping the distribution of density function for membrane vibrations [15] and acoustics [16], and plate [17,18]. Nevertheless, spurious eigensolutions are inherent in the imaginary-part BEM, the real-part BEM and the MRM. Numerically speaking, the spurious eigensolutions result from the rank deficiency of the influence coefficient matrix. This implies the fewer number of constraint equations making the solution space larger. Mathematically speaking, the spurious eigensolutions for interior problems arise from the same source of `` improper approximation of the null space of operator''. Two sources of rank deficiency in the influence matrices can be classified, one is spurious solution due to incompleteness and the other is due to the nontrivial eigensolution.

In this paper, we will employ the imaginary-part fundamental solution as RBF to solve the plate vibration problems. The main difference between the present formulation and the method of fundamental solution is that we adopt only the imaginary-part fundamental solution instead of employing the complex-valued singular kernel. In solving the problem numerically, elements are not required and only boundary nodes are necessary. Both the boundary and source points are distributed on the boundary only. The difference between the present method and the NDIF method will be emphasized in selecting the interpolation bases. The occurrence of spurious eigenvalues will be discussed. For the case of circular plate, the eigensolutions will be analytically derived in the discrete system by using circulants. In addition, the true eigenvalues and eigen modes for a circular plate will be derived exactly by using degenerate kernel and Fourier series expansion. Two examples, circular plates subject to the clamped and simply-supported boundary conditions, will be demonstrated to see the validity of the present formulation.

Meshless formulation using radial basis function of the imaginary-part fundamental solution

The governing equation for a free flexural vibration of a uniform thin plate is written as follows:

$$\nabla^4 w(x) = l^4 w(x),\ x \in \Omega, \tag{1}$$

where w is the lateral displacement, $l^4 = \frac{w^2 r h}{D}$, λ is the frequency parameter, w is the circular frequency, ρ is the surface density, D is the flexural rigidity expressed as $D = \frac{Eh^3}{12(1-n)}$ in terms of Young's modulus E, the Poisson ratio ν and the plate thickness h, and O is the domain of the thin plate.

The radial basis function is defined by

$$G(x,s) = j\,(|\,s - x\,|) \tag{2}$$

where x and s are the collocation and source points, respectively. The Euclidean norm $|\,s - x\,|$ is referred to as the radial distance between the collocation and source points. The two-point function $(\,j\,(|\,s - x\,|)\,)$ is called the RBF since it depends on the radial distance between x and s. By considering the imaginary-part fundamental solution ($W(s,x) = \mathrm{Im}\{\frac{i}{8l^2}(H_0^{(2)}(lr) + H_0^{(1)}(ilr))\}$) [19] for the plate vibration, the six kernels in the dual formulation are

$$W(s,x) = \frac{1}{8l^2}(J_0(lr) + I_0(lr)), \tag{3}$$

$$\Theta(s,x) = \frac{\partial W(s,x)}{\partial n_s} = \frac{1}{8l}\frac{-J_1(lr) + I_1(lr)}{r} y_i n_i, \tag{4}$$

$$W_n(s,x) = \frac{\partial W(s,x)}{\partial n_x} = \frac{1}{8l}\frac{J_1(lr) - I_1(lr)}{r} y_i \bar{n}_i, \tag{5}$$

$$\Theta_n(s,x) = \frac{\partial^2 W(s,x)}{\partial n_s \partial n_x} = \frac{1}{8l}\left(\frac{-lJ_2(lr) - lI_2(lr)}{r^2} y_i n_i y_j \bar{n}_j + \frac{J_1(lr) - I_1(lr)}{r} n_i \bar{n}_i\right), \tag{6}$$

$$W_{nn}(s,x) = \frac{\partial^2 W(s,x)}{\partial n_x \partial n_x} = \frac{1}{8l}\left(\frac{lJ_2(lr) + lI_2(lr)}{r^2} y_i \bar{n}_i y_j \bar{n}_j + \frac{-J_1(lr) + I_1(lr)}{r} \bar{n}_i \bar{n}_i\right), \tag{7}$$

$$\begin{aligned}\Theta_{nn}(s,x) = \frac{\partial^3 W(s,x)}{\partial n_s (\partial n_x)^2} = \frac{1}{8}\Bigg(&\frac{-lJ_3(lr) + lI_3(lr)}{r^3} y_i n_i y_j \bar{n}_j y_k \bar{n}_k + \frac{J_2(lr) + I_2(lr)}{r^2} y_j \bar{n}_j n_i \bar{n}_i \\ &+ \frac{J_2(lr) + I_2(lr)}{r^2} y_i n_i \bar{n}_j \bar{n}_j + \frac{J_2(lr) + I_2(lr)}{r^2} y_k \bar{n}_k n_i \bar{n}_i\Bigg),\end{aligned} \tag{8}$$

in which $r \equiv |\,s - x\,|$ is the distance between the source and collocation points; n_i is the ith component of the outnormal vector at s; $\bar{n}_i$ is the ith component of the outnormal vector at x, J_m and I_m denote the first kind of the mth order Bessel and modified Bessel functions, respectively, and $y_i \equiv |\,s_i - x_i\,|$, i= 1, 2, are the differences of the ith components of s and x, respectively. Based on the six kernels, the displacement, slope and moment can be represented by

$$w(x) = \sum_{j=1}^{2N} W(s_j,x)p(s_j) + \sum_{j=1}^{2N} \Theta(s_j,x)q(s_j), \quad x \in \Omega \tag{9}$$

$$q(x) = \sum_{j=1}^{2N} W_n(s_j,x)p(s_j) + \sum_{j=1}^{2N} \Theta_n(s_j,x)q(s_j), \quad x \in \Omega \tag{10}$$

$$m(x) = \sum_{j=1}^{2N} W_m(s_j,x)p(s_j) + \sum_{j=1}^{2N} \Theta_m(s_j,x)q(s_j), \quad x \in \Omega \tag{11}$$

where, $W_m(s_j, x) = W_{nn}(s_j, x) + \frac{n}{r} W_n(s_j, x)$ and $\Theta_m(s_j, x) = \Theta_{nn}(s_j, x) + \frac{n}{r}\Theta_n(s_j, x)$, $p(s_j)$ and $q(s_j)$ are the generalized unknowns at s_j, $2N$ is the number of collocation points. The main difference between the present formulation and the NDIF method proposed by Kang and Lee [14] is the choice of RBF. The NDIF method chose $W(s, x) = J_0(lr)$ and $\Theta(s, x) = I_0(lr)$. A comparison between the Kang method and our approach is shown in Table 1. After collocating the point x on the boundary, the boundary conditions of the clamped plate are

$$\{0\} = [W]\{p\} + [\Theta]\{q\}, \quad w(x) = 0, \tag{12}$$

$$\{0\} = [W_n]\{p\} + [\Theta_n]\{q\}, \quad q(x) = 0, \tag{13}$$

where $\{p\}$ and $\{q\}$ are the vectors of undetermined coefficients. By assembling Eqs.(12) and (13) together, we have

$$[SM]\begin{Bmatrix} p \\ q \end{Bmatrix} = \{0\}, \tag{14}$$

where

$$[SM] = \begin{bmatrix} W & \Theta \\ W_n & \Theta_n \end{bmatrix}_{4N\times 4N}, \tag{15}$$

the determinant of the matrix versus eigenvalue must become zero to obtain the nontrivial solution, i.e.,

$$\det[SM] = 0. \tag{16}$$

By plotting the determinant versus the frequency parameter, the curve drops at the positions of eigenvalues. Similarly, the simply-supported case can be obtained.

Analytical study for the eigensolution of a circular plate using circulants in the discrete system

For the circular plate, we can express $x = (r, f)$ and $s = (R, q)$ in terms of polar coordinate. The W kernels can be expressed in terms of degenerate kernels as shown below:

$$W(s,x) = \begin{cases} W^I(q,f) = \dfrac{1}{8l^2}\displaystyle\sum_{m=-\infty}^{\infty}[J_m(lR)J_m(lr) + (-1)^m I_m(lR)I_m(lr)]\cos(m(q-f)), & R > r \\ W^E(q,f) = \dfrac{1}{8l^2}\displaystyle\sum_{m=-\infty}^{\infty}[J_m(lr)J_m(lR) + (-1)^m I_m(lr)I_m(lR)]\cos(m(q-f)), & R < r \end{cases} \tag{17}$$

where the superscripts "I" and "E" denote the interior (R > ?) and exterior domains (R < ?), respectively. Since the rotation symmetry is preserved for a circular boundary, the six influence matrices in Eqs.(9)-(11) are denoted by $[W]$, $[T]$, $[W_n]$, $[T_n]$, $[W_m]$ and $[T_m]$ of the circulants with the elements,

$$K_{ij} = K(r, q_j; r, f_i), \tag{18}$$

where the kernel K can be W, Θ, W_n, Θ_n, , W_m or Θ_m, f_i and q_j are the angles of observation and boundary points, respectively. By superimposing $2N$ lumped strength along the boundary, we have the influence matrices,

$$[K] = \begin{bmatrix} a_0 & a_1 & a_2 & \cdots & a_{2N-2} & a_{2N-1} \\ a_{2N-1} & a_0 & a_1 & \cdots & a_{2N-3} & a_{2N-2} \\ a_{2N-2} & a_{2N-1} & a_0 & \cdots & a_{2N-4} & a_{2N-3} \\ \vdots & \vdots & \vdots & \ddots & \vdots & \vdots \\ a_1 & a_2 & a_3 & \cdots & a_{2N-1} & a_0 \end{bmatrix} \tag{19}$$

where the elements of the first row can be obtained by

$$a_{j-i} = K(s_j, x_i)\ . \tag{20}$$

The matrix [*K*] in Eq.(19) is found to be a circulant [20] since the rotational symmetry for the influence coefficients is considered. By using the degenerate kernel and the orthogonal property, the eigenvalue of the matrices [*W*], [*T*], [W_n], [T_n], [W_m] and [T_m] can be respectively obtained as follows:

$$l_\ell = \frac{N}{4l^2}[J_\ell(l r)J_\ell(l r) + (-1)^\ell I_\ell(l r)I_\ell(l r)], \tag{21}$$

$$m_\ell = \frac{N}{4l}[J_\ell(l r)J_l{}'(l r) + (-1)^\ell I_\ell(l r)I_\ell{}'(l r)], \tag{22}$$

$$n_\ell = \frac{N}{4l}[J_\ell{}'(l r)J_\ell(l r) + (-1)^\ell I_\ell{}'(l r)I_\ell(l r)], \tag{23}$$

$$d_\ell = \frac{N}{4}[J_\ell{}'(l r)J_\ell(l r) + (-1)^\ell I_\ell{}'(l r)I_\ell(l r)], \tag{24}$$

$$k_\ell = \frac{N}{4}[J_\ell{}''(l r)J_\ell(l r) + (-1)^\ell I_\ell{}''(l r)I_\ell(l r)] + \frac{Nn}{4l r}[J_\ell{}'(l r)J_\ell(l r) + (-1)^\ell I_\ell{}'(l r)I_\ell(l r)], \tag{25}$$

$$h_\ell = \frac{Nl}{4}[J_\ell{}''(l r)J_\ell{}'(l r) + (-1)^\ell I_\ell{}''(l r)I_\ell{}'(l r)] + \frac{Nn}{4r}[J_\ell{}'(l r)J_\ell{}'(l r) + (-1)^\ell I_\ell{}'(l r)I_\ell{}'(l r)], \tag{26}$$

where $\ell = 0, \pm 1, \pm 2, \cdots, \pm(N-1), N$. Since the matrix [*W*] is a symmetric circulant, it can be expressed by

$$[W] = \Phi \Sigma_W \Phi^T = \Phi \begin{bmatrix} l_0 & 0 & 0 & \cdots & 0 & 0 & 0 \\ 0 & l_1 & 0 & \cdots & 0 & 0 & 0 \\ 0 & 0 & l_{-1} & \cdots & 0 & 0 & 0 \\ \vdots & \vdots & \vdots & \ddots & \vdots & \vdots & \vdots \\ 0 & 0 & 0 & \cdots & l_{(N-1)} & 0 & 0 \\ 0 & 0 & 0 & \cdots & 0 & l_{-(N-1)} & 0 \\ 0 & 0 & 0 & \cdots & 0 & 0 & l_N \end{bmatrix}_{2N \times 2N} \Phi^T, \tag{27}$$

where

$$\Phi = \frac{1}{\sqrt{2N}} \begin{bmatrix} 1 & 1 & 0 & \cdots & 1 & 0 & 1 \\ 1 & \cos(\frac{2p}{2N}) & \sin(\frac{2p}{2N}) & \cdots & \cos(\frac{2p(N-1)}{2N}) & \sin(\frac{2p(N-1)}{2N}) & \cos(\frac{2pN}{2N}) \\ 1 & \cos(\frac{4p}{2N}) & \sin(\frac{4p}{2N}) & \cdots & \cos(\frac{4p(N-1)}{2N}) & \sin(\frac{4p(N-1)}{2N}) & \cos(\frac{4pN}{2N}) \\ \vdots & \vdots & \vdots & \ddots & \vdots & \vdots & \vdots \\ 1 & \cos(\frac{2p(2N-2)}{2N}) & \sin(\frac{2p(2N-2)}{2N}) & \cdots & \cos(\frac{p(4N-4)(N-1)}{2N}) & \sin(\frac{p(4N-4)(N-1)}{2N}) & \cos(\frac{p(4N-4)(N)}{2N}) \\ 1 & \cos(\frac{2p(2N-1)}{2N}) & \sin(\frac{2p(2N-1)}{2N}) & \cdots & \cos(\frac{p(4N-2)(N-1)}{2N}) & \sin(\frac{p(4N-2)(N-1)}{2N}) & \cos(\frac{p(4N-2)(N)}{2N}) \end{bmatrix}_{2N \times 2N} \tag{28}$$

Similarly, [*T*], [W_n], [T_n], [W_m] and [T_m] can be decomposed. Equation (15) can be reduced to

$$[SM]=\begin{bmatrix}\Phi\Sigma_W\Phi^T & \Phi\Sigma_\Theta\Phi^T\\ \Phi\Sigma_{W_n}\Phi^T & \Phi\Sigma_{\Theta_n}\Phi^T\end{bmatrix}_{4N\times 4N}, \tag{29}$$

Eq.(29) can be reformulated into

$$[SM]=\begin{bmatrix}\Phi & 0\\ 0 & \Phi\end{bmatrix}\begin{bmatrix}\Sigma_W & \Sigma_\Theta\\ \Sigma_{W_n} & \Sigma_{\Theta_n}\end{bmatrix}\begin{bmatrix}\Phi & 0\\ 0 & \Phi\end{bmatrix}^T, \tag{30}$$

Since F is orthogonal, the determinant of $[SM]_{4N\times 4N}$ is

$$\det[SM]=s_0(s_1 s_2\cdots s_{N-1})^2 s_N, \tag{31}$$

where

$$s_\ell = l_\ell d_\ell - m_\ell n_\ell = \frac{N}{4}\frac{[J_\ell'(lr)I_\ell(lr)-I_\ell'(lr)J_\ell(lr)]^2}{J_\ell(lr)J_\ell(lr)+(-1)^\ell I_\ell(lr)I_\ell(lr)} \tag{32}$$

for the clamped case. After using the differential property of Bessel function, Equation (32) can be reduced to

$$\frac{[J_\ell(lr)I_{\ell+1}(lr)+I_\ell(lr)J_{\ell+1}(lr)]^2}{J_\ell(lr)J_\ell(lr)+(-1)^\ell I_\ell(lr)I_\ell(lr)}=0,\quad \ell=0,\pm1,\pm2,\cdots,\pm(N-1),\ N, \tag{33}$$

According to Eq.(33), the eigensolution is found to match the exact solution well since the denominator is never zero. The true eigen equation is

$$J_\ell(lr)I_{\ell+1}(lr)+I_\ell(lr)J_{\ell+1}(lr)=0 \tag{34}$$

Similarly, the eigen equation of simply-supported plate can be obtained as follows:

$$(J_\ell(lr)I_{\ell+1}(lr)+I_\ell(lr)J_{\ell+1}(lr))\left(\frac{I_{\ell+1}(lr)}{I_\ell(lr)}+\frac{J_{\ell+1}(lr)}{J_\ell(lr)}-\frac{2lr}{(1-n)}\right)=0,$$
$$\ell=0,\pm1,\pm2,\cdots,\pm(N-1),\ N, \tag{35}$$

It is interesting to find that the eigensolution of the clamped case is embedded in the Eq.(35) for the simply-supported case. After comparing with the exact solution, the present method results in spurious eigensolution $[J_\ell(lr)I_{\ell+1}(lr)+I_\ell(lr)J_{\ell+1}(lr)]=0$ at the same time when we obtain the true eigen equation

$$\frac{I_{\ell+1}(lr)}{I_\ell(lr)}+\frac{J_{\ell+1}(lr)}{J_\ell(lr)}=\frac{2lr}{(1-n)}, \tag{36}$$

for the simply-supported case.

Derivation of interior modes for the circular plate using degenerate kernel and Fourier series in the continuous system

Derivation of the eigenequation

For the purpose of analytical study, we use the continuous system to obtain the eigenequation. The unknowns densities $p(s)$ and $q(s)$, can be expanded into Fourier series by

$$p(s)=a_0+\sum_{n=1}^{\infty}(a_n\cos(nq)+b_n\sin(nq)),\quad s\in B, \tag{37}$$

$$q(s)=c_0+\sum_{n=1}^{\infty}(c_n\cos(nq)+d_n\sin(nq)),\quad s\in B, \tag{38}$$

where a_n, b_n, c_n and d_n are the undetermined Fourier coefficients. The field representations of Eqs.(9)-(11) are written as

$$w(x) = \int_B W^E(s,x)\,p(s)dB(s) + \int_B \Theta^E(s,x)q(s)dB(s) \tag{39}$$

$$q(x) = \int_B W_n^E(s,x)\,p(s)dB(s) + \int_B \Theta_n^E(s,x)q(s)dB(s) \tag{40}$$

$$m(x) = \int_B W_m^E(s,x)\,p(s)dB(s) + \int_B \Theta_m^E(s,x)q(s)dB(s) \tag{41}$$

For the clamped case, we have

$$0 = \int_0^{2p} W^E(s,x)\,(a_0 + \sum_{n=1}^{\infty}(a_n\cos(nq) + b_n\sin(nq)))\,r\,dq$$
$$+ \int_0^{2p} \Theta^E(s,x)\,(c_0 + \sum_{n=1}^{\infty}(c_n\cos(nq) + d_n\sin(nq)))\,r\,dq\,, \quad x \in B, \tag{42}$$

$$0 = \int_0^{2p} W_n^E(s,x)\,(a_0 + \sum_{n=1}^{\infty}(a_n\cos(nq) + b_n\sin(nq)))\,r\,dq$$
$$+ \int_0^{2p} \Theta_n^E(s,x)\,(c_0 + \sum_{n=1}^{\infty}(c_n\cos(nq) + d_n\sin(nq)))\,r\,dq\,, \quad x \in B, \tag{43}$$

By substituting the degenerate kernels and employing the orthogonality condition of the Fourier series, the Fourier coefficients a_n, b_n, c_n and d_n satisfy

$$c_n = -\frac{1}{l}\frac{J_n(lr)J_n(lr) + (-1)^n I_n(lr)I_n(lr)}{J_n'(lr)J_n(lr) + (-1)^n I_n'(lr)I_n(lr)}a_n, \quad n = 0, 1, 2, \cdots, \tag{44}$$

$$d_n = -\frac{1}{l}\frac{J_n(lr)J_n(lr) + (-1)^n I_n(lr)I_n(lr)}{J_n'(lr)J_n(lr) + (-1)^n I_n'(lr)I_n(lr)}b_n, \quad n = 0, 1, 2, \cdots, \tag{45}$$

From Eq. (43) we similarly have

$$c_n = -\frac{\frac{1}{8}(J_n''(lr)J_n(lr) + (-1)^n I_n''(lr)I_n(lr)) + \frac{n}{8rl}(J_n'(lr)J_n(lr) + (-1)^n I_n'(lr)I_n(lr))}{\frac{l}{8}(J_n''(lr)J_n'(lr) + (-1)^n I_n''(lr)I_n'(lr)) + \frac{n}{8rl}(J_n'(lr)J_n'(lr) + (-1)^n I_n'(lr)I_n'(lr))}a_n,$$
$$n = 0, 1, 2, \cdots, \tag{46}$$

$$d_n = -\frac{\frac{1}{8}(J_n''(lr)J_n(lr) + (-1)^n I_n''(lr)I_n(lr)) + \frac{n}{8rl}(J_n'(lr)J_n(lr) + (-1)^n I_n'(lr)I_n(lr))}{\frac{l}{8}(J_n''(lr)J_n'(lr) + (-1)^n I_n''(lr)I_n'(lr)) + \frac{n}{8rl}(J_n'(lr)J_n'(lr) + (-1)^n I_n'(lr)I_n'(lr))}b_n,$$
$$n = 0, 1, 2, \cdots, \tag{47}$$

To seek nontrivial data for the generalized coefficients of a_n, b_n,, c_n and d_n, we obtain the eigenequations

$$(J_\ell'(lr)I_n(lr) - I_\ell'(lr)J_n(lr))^2 = (J_n(lr)I_{n+1}(lr) + I_n(lr)J_{n+1}(lr))^2 = 0 \tag{48}$$

for the clamped case. Similarly, we can obtain the eigenequation

$$[J_\ell(lr)I_{\ell+1}(lr) + I_\ell(lr)J_{\ell+1}(lr)][\frac{I_{\ell+1}(lr)}{I_\ell(lr)} + \frac{J_{\ell+1}(lr)}{J_\ell(lr)} - \frac{2lr}{(1-n)}] = 0\,, \tag{49}$$

for the simply-supported case. The eigenequation in Eq.(49) is the same with Eq.(35) obtained by using circulants in the discrete system.

Derivation of the eigenmode

By substituting the degenerate kernels for the interior point (0 < r < ?) and the relationships of Eqs.(44) and (45) between the generalized coefficients of $p(s)$ and $q(s)$ into Eq.(9) for the clamped case, we have

$$w_n(r,f) = (J_n(l r)I_{n+1}(l r) + I_n(l r)J_{n+1}(l r))$$

$$(-1)^n \frac{J_n(l r)I_n(l r) - I_n(l r)J_n(l r)}{J_n(l r)J_{\ell}'(l r) + (-1)^n I_n(l r)I_{\ell}'(l r)}(a_n \cos(nf) + b_n \sin(nf)),$$

$$n = 1, 2, 3, \cdots, 0 < r < r, 0 \leq f < 2p. \quad (50)$$

Similar, we can obtain the eigenmode of the simply-supported case. It is interesting to find that the eigen mode of the clamped and simply-supported cases are very similar. However, the numerical results in the contour plots are different since different eigenvalues are used.

Numerical results and discussions

A circular plate with a radius (? = 1) subjected to the clamped ($w(x)$ = 0 and ?(x) = 0) and simply-supported ($w(x)$ = 0 and $m(x)$ = 0) boundary conditions are considered, respectively. In the first case, analytical solutions of eigenequation and eigenmode are shown in Eqs.(34) and (50). To compare with the Kang and Lee's results [14], Fig.1 shows the determinant of [SM] versus ? using the present method of continuous and discrete formulations. The eigenvalues agree well with the analytical solution. In order to verify our finding, Fig.2 is shows the determinant of [SM] versus ? using the present method for both clamped and simply-supported plates. The eigensolution of simply-supported plate is contaminated by the true eigensolution of clamped case. The numerical results match well with our prediction using continuous and discrete formulation. The former six interior modes obtained are shown in Fig.3.

Conclusions

We have developed a meshless method for the vibration problem of clamped and simply-supported plates by using the imaginary-part kernel, which was chosen as the RBF to approximate the solution. Neither boundary elements nor singularities are required. It is interesting to find that spurious eigensolution of simply-supported case appears to be the true eigensolution of the clamped case. In addition, the eigenfunction of clamped and simply-supported are of the same form but different eigenvalues. For a circular plate, the eigenvalue, boundary mode and interior mode were derived analytically by using the degenerate kernel, Fourier series and circulants. Circular plates subject to the clamped and simply-supported boundary conditions, were demonstrated analytically and numerically to check the validity of the meshless formulation.

Acknowledgments

Financial support from the National Science Council under Grant No. NSC-90-2211-E-019-006 for National Taiwan Ocean University is gratefully acknowledged.

References

[1] Belystcho T, Lu Y, Gu L, "Element free Galerkin methods." International Journal for Numerical Methods in Engineering 1994;37:229-56.
[2] Liu WK, Jun S, Zhang YF, "Reproducing kernel particle methods." International Journal for Numerical Methods in Engineering 1995;20:1081-106.
[3] Mukherjee YX, Mukherjee S, "The boundary node method for potential problems." International Journal for Numerical Methods in Engineering 1997;40:797-815.
[4] Atluri SN, Zhu T, "A new meshless local Petrov-Galerkin (MLPG) approach in computational mechanics." Computational Mechanics 1998;22:117-27.
[5] Sladek V, Sladek J, Atluri SN, and Van Keer R, "Numerical integration of singularities in meshless implementation of local boundary integral equations." Computational Mechanics 2000;25:394-403.
[6] Golberg MA, Chen CS, Ganesh M, "Particular solutions of 3D Helmholtz-type equations using compactly supported radial basis functions." Engineering Analysis with Boundary Element 2000;24:539-47.
[7] Banerjee PK, Ahmad S, Wang HC, "A new BEM formulation for the acoustic eigenfrequency analysis." International Journal for Numerical Methods in Engineering 1998;26:1299-309.
[8] Chen JT, Kuo SR, Chen KH, "A nonsingular integral formulation for the Helmholtz eigenproblems of a circular domain." Journal of the Chinese Instiute of Engineers 1999;22(6):729-39.
[9] Kamiya N, Ando E, Nogae K, "A new complex-valued formulation and eigenvalue analysis of the Helmholtz equation by boundary element method." Advances in Engineering Software 1996;26:219-27.
[10] Tai GRG, Shaw RP, "Helmholtz equation eigenvalues and eigenmodes for arbitrary domains." Journal of the Acoustical Society of America 1974;56:796-804.
[11] De Mey G, "A simplified integral equation method for the calculation of the eigenvalues of Helmholtz equation." International Journal for Numerical Methods in Engineering 1977;11:1340-42.
[12] Kang SW, Lee JM, "Application of free vibration analysis of membranes using the non-dimensional dynamic influence function." Journal of Sound and Vibration 2000;234(3):455-70.
[13] Kang SW, Lee JM, "Eigenmode analysis of arbitrarily shaped two-dimensional cavities by the method of point matching." Journal of Acoustical Society of America 2000;107(3):1153-60.
[14] Kang SW, Lee JM, "Free vibration analysis of arbitrary shaped plates with clamped edges using wave-type functions." Journal of Sound and Vibration 2001;242(1):9-26.
[15] Chen JT, Kuo SR, Chen KH, Cheng YC, Comments on "Vibration analysis of arbitrary shaped membranes using non-dimensional dynamic influence function." Journal of Sound and Vibration 2000;235(1):156-71.
[16] Chen JT, Chang MH, Chung IL, Cheng YC, Comments on "Eigenmode analysis of arbitrarily shaped two-dimensional cavities by the method of point matching." Journal of Acoustical Society of America 2002;111(1):33-36.
[17] Chen JT, Chen IL, Chen KH, Lee YT, Comment on "Free vibration analysis of arbitrarily shaped plates with clamped edges using wave-type function". Journal of Sound and Vibration 2002; Accepted.
[18] Chen JT, Chen IL, Chen KH, Yeh YT, Lee YT, A meshless method for free vibration analysis of arbitrarily shaped plates with clamped boundaries using radial basis function. Engineering Analysis with Boundary Elements 2002, Accepted.
[19] Kitahara M, "Boundary integral equation methods in eigenvalue problems of elastodynamics and thin plates." Amsterdam: Elsevier, 1985.
[20] Goldberg JL, "Matrix Theory with Applications." New York: McGraw-Hill, 1991.

Table 1. Comparisons of the NDIF method and present method.

	NDIF method		Present method	
Radial basis function (RBF)	$W(s,x)=J_0(lr)$ $\Theta(s,x)=I_0(lr)$		$W(s,x)=\frac{1}{8l^2}(J_0(lr)+I_0(lr))$ $\Theta(s,x)=\frac{\partial W(s,x)}{\partial n_s}$	
Clamped plate	$J_\ell(lr)I_{\ell+1}(lr)+J_{\ell+1}(lr)I_\ell(lr)=0$	(True)	$J_\ell(lr)I_{\ell+1}(lr)+J_{\ell+1}(lr)I_\ell(lr)=0$	(True)
	$J_\ell(lr)=0$	(Spurious)	No	(Spurious)
Simply-supported plate	$\frac{I_{\ell+1}(lr)}{I_\ell(lr)}+\frac{J_{\ell+1}(lr)}{J_\ell(lr)}=\frac{2lr}{(1-n)}$	(True)	$\frac{I_{\ell+1}(lr)}{I_\ell(lr)}+\frac{J_{\ell+1}(lr)}{J_\ell(lr)}=\frac{2lr}{(1-n)}$	(True)
	$J_\ell(lr)=0$	(Spurious)	$J_\ell(lr)I_{\ell+1}(lr)+J_{\ell+1}(lr)I_\ell(lr)=0$	(Spurious)
Treatment	Net approach		CHEEF method Dual formulation with SVD updating	

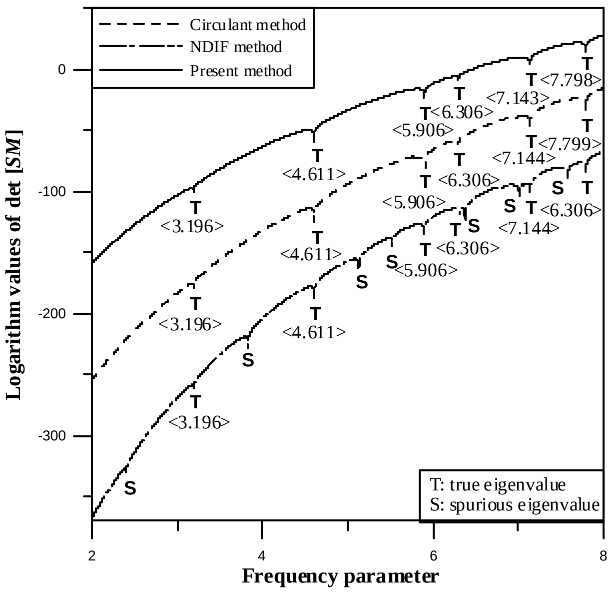

Fig.1

Logarithm curve for $det[SM_N]$ versus frequency parameter of the circular clamped plate using the different methods.

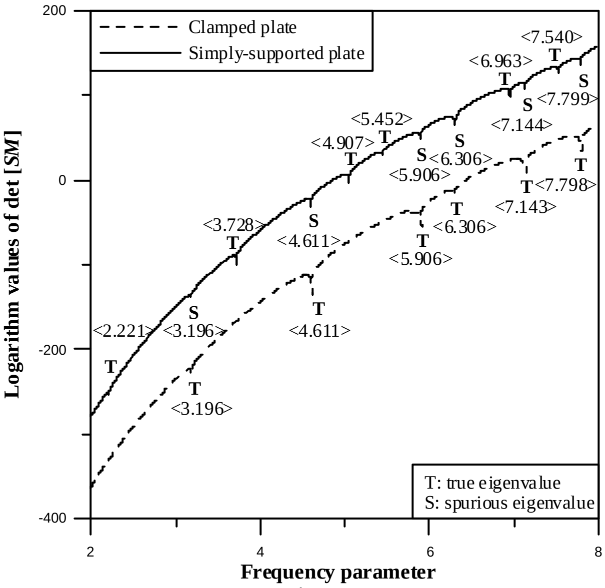

Fig.2

Logarithm curve for $det[SM_N]$ versus frequency parameter of the circular clamped and simply-supported plate using the present methods.

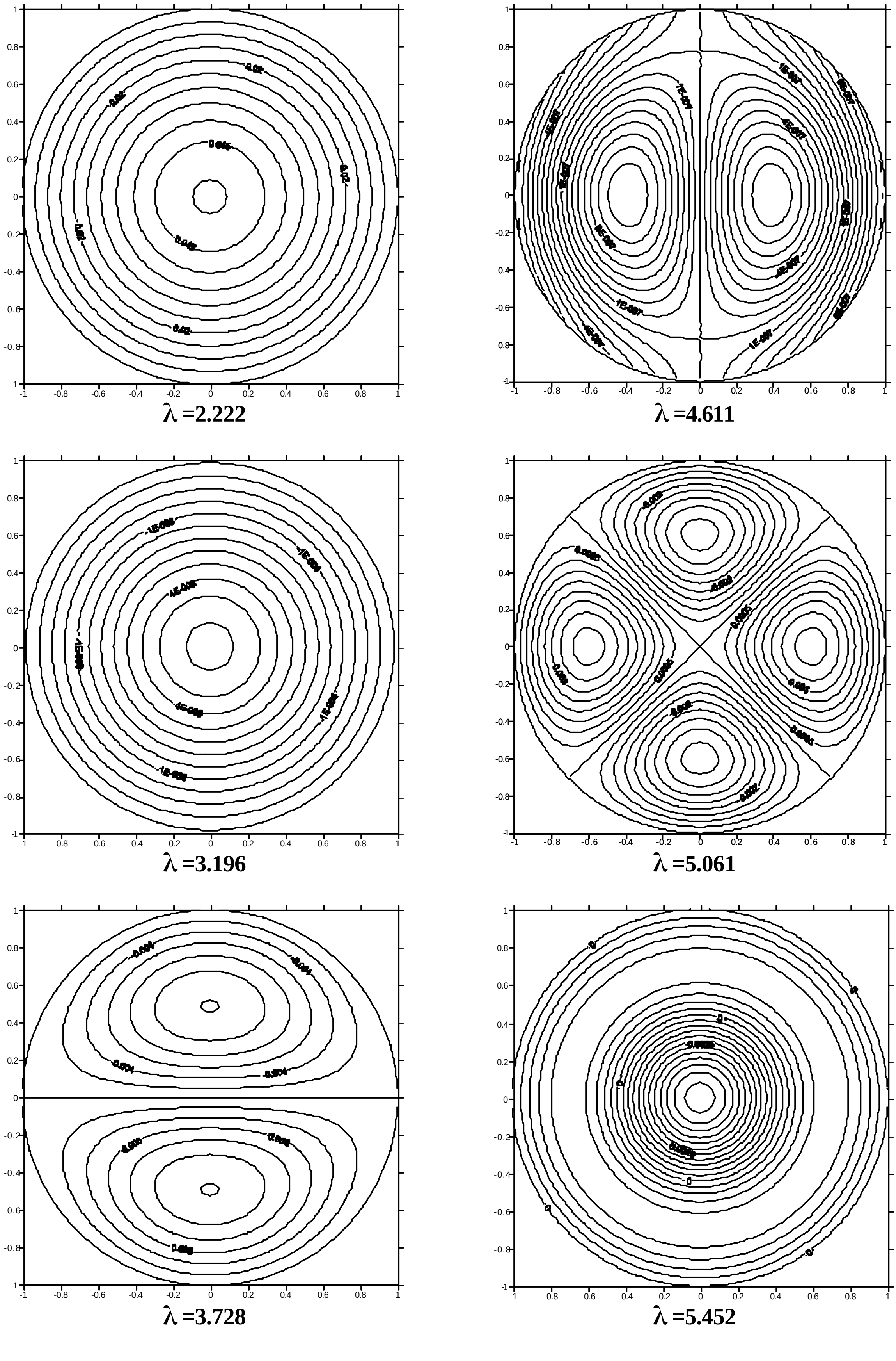

Fig.3 The former six modes for the simply-supported circular plate using the present method.

無網格法配合徑向基底函數於任意外形板振動之分析

李應德[1]　陳義麟[2]　陳桂鴻[3]　陳正宗[4]

[1]國立臺灣海洋大學河海工程學系研究生
[2]國立高雄海洋技術學院造船工程系副教授
[3]國立臺灣海洋大學河海工程學系博士候選人
[4]國立臺灣海洋大學河海工程學系教授

摘要

本文是使用無網格法配合徑向基底函數來求解固定及簡支承邊界板之特徵頻率，其中影響係數矩陣可輕易的由徑向基底函數求得。利用虛部基本解當徑向基底函數求解發現假根常常會伴隨著真根產生，更有趣的是我們從中發現到固定邊界板振動問題之真根竟然是簡支承板振動問題之假根。為了同時求得特徵值及邊界模態，我們在計算的過程中運用了奇異值分解法來求解，文中我們以圓形板為例來論證我們的發現。

關鍵詞：無網格法、徑向基底函數、板振動、固定邊界、簡支承邊界